

Evidence for Entropy Effects in the Reduction of Ceria–Zirconia Solutions

Parag R. Shah,[†] Taeyoon Kim,[†] Gong Zhou,[†] Paolo Fornasiero,[‡] and Raymond J. Gorte^{*†}

Department of Chemical and Biomolecular Engineering, University of Pennsylvania, Philadelphia, Pennsylvania 19104, and Chemistry Department, INSTM – Trieste RU and Centre of Excellence for Nanostructured Materials, University of Trieste, Via L. Giorgieri 1, I-34127 Trieste, Italy

Received June 13, 2006. Revised Manuscript Received August 18, 2006

An instrument for Coulometric-titration measurements was built and used to measure the thermodynamic redox properties for a 10 wt % Cu/silica catalyst at 973 K and for two ceria–zirconia solid solutions, $\text{Ce}_{0.81}\text{Zr}_{0.19}\text{O}_2$ and $\text{Ce}_{0.25}\text{Zr}_{0.75}\text{O}_2$, between 873 and 1073 K. For Cu/silica, the equilibrium data show two well-defined steps in the oxygen isotherms, associated with equilibrium between Cu and Cu_2O and between Cu_2O and CuO; and the $P(\text{O}_2)$ associated with these two steps are in close agreement with values expected for pure Cu. The oxidation enthalpies for both $\text{Ce}_{0.81}\text{Zr}_{0.19}\text{O}_2$ and $\text{Ce}_{0.25}\text{Zr}_{0.75}\text{O}_2$ were similar, between -500 and -550 kJ/mol of O_2 , and independent of the extent of reduction. However, there is a step change in $-\Delta S$ of reduction for $\text{Ce}_{0.81}\text{Zr}_{0.19}\text{O}_2$, from ~ 250 to < 100 J/mol·K, after removal of approximately one oxygen for every two Zr^{4+} . A model is presented which views the reduction of ceria–zirconia as removal of oxygen from “pyrochlore-like” structures, with some of the changes in reducibility associated with the number of sites from which oxygen can be removed.

Introduction

Ceria–zirconia solutions are widely used for oxygen-storage capacitance (OSC) in automobiles,^{1–4} and ceria-based catalysts are finding new catalytic applications as supports for water–gas shift^{5–12} and reforming catalysts^{13,14} and for hydrocarbon-oxidation catalysts in diesel emissions control systems.^{15–17} The role of ceria in each of these applications almost certainly involves oxidation and reduction of ceria.

However, while thermodynamic data for oxidation and reduction of bulk ceria are available,^{18–25} there is little analogous information on ceria–zirconia mixed oxides, even though these materials are well-known to be more easily reduced than pure ceria. Therefore, our laboratories have begun to investigate the equilibrium redox properties of ceria–zirconia solid solutions to quantify differences between ceria and the mixed oxides and to determine how composition and structure affect these differences.²⁶

The most reliable means for obtaining thermodynamic, redox properties for oxides is from the equilibrium constants which can be determined from the O_2 fugacity, $P(\text{O}_2)$, that is in equilibrium with the oxidized and reduced phases. For example, the equilibrium constant for the reaction $\text{Cu}_2\text{O} \rightleftharpoons \text{Cu} + \frac{1}{2}\text{O}_2$ is equal to $P(\text{O}_2)^{1/2}$ when Cu and Cu_2O are both present. Because the free-energy change for reduction of $\text{CeO}_{(2-x)}$ is a function of x ,^{18–25} the value of $P(\text{O}_2)^{1/2}$ that is in equilibrium with a particular ceria composition can be

* Corresponding author. Phone: 215-898-4439. Fax: 215-573-2093. E-mail: gorte@seas.upenn.edu.

[†] University of Pennsylvania.

[‡] University of Trieste.

- (1) Kaspar, J.; Fornasiero, P.; Hickey, N. *Catal. Today* **2003**, *77*, 419–449.
- (2) McCabe, R. W.; Kisenyi, J. M. *Chem. Ind.* **1995**, 605–608.
- (3) Shelef, M.; Graham, G. W.; McCabe, R. W. In *Catalysis by Ceria and Related Materials*; Trovarelli, A., Ed.; Imperial College Press: London, 2002.
- (4) Sugiura, M.; Ozawa, M.; Suda, A.; Suzuki, T.; Kanazawa, T. *Bull. Chem. Soc. Jpn.* **2005**, *78*, 752–767.
- (5) Bunluesin, T.; Gorte, R. J.; Graham, G. W. *Appl. Catal., B* **1998**, *15*, 107–114.
- (6) Choung, S. Y.; Ferrandon, M.; Krause, T. *Catal. Today* **2005**, *99*, 257–262.
- (7) Fu, Q.; Saltsburg, H.; Flytzani-Stephanopoulos, M. *Science* **2003**, *301*, 935–938.
- (8) Ghenciu, A. F. *Curr. Opin. Solid State Mater. Sci.* **2002**, *6*, 389–399.
- (9) Hilaire, S.; Wang, X.; Luo, T.; Gorte, R. J.; Wagner, J. *Appl. Catal., A* **2001**, *215*, 271–278.
- (10) Jacobs, G.; Patterson, P. A.; Graham, U. M.; Sparks, D. E.; Davis, B. H. *Appl. Catal., A* **2004**, *269*, 63–73.
- (11) Liu, X. S.; Ruettinger, W.; Xu, X. M.; Farrauto, R. *Appl. Catal., B* **2005**, *56*, 69–75.
- (12) Swartz, S. L.; Seabaugh, M. M.; Holt, C. T.; Dawson, W. J. *Fuel Cell Bull.* **2001**, *4*.
- (13) Craciun, R.; Shereck, B.; Gorte, R. J. *Catal. Lett.* **1998**, *51*, 149–153.
- (14) Farrauto, R.; Hwang, S.; Shore, L.; Ruettinger, W.; Lampert, J.; Giroux, T.; Liu, Y.; Ilinich, O. *Annu. Rev. Mater. Res.* **2003**, *33*, 1–27.
- (15) Bueno-Lopez, A.; Krishna, K.; Makkee, M.; Moulijn, J. *Catal. Lett.* **2005**, *99*, 203–205.

- (16) Bueno-Lopez, A.; Krishna, K.; Makkee, M.; Moulijn, J. A. J. *Catal.* **2005**, *230*, 237–248.
- (17) Heck, R. M.; Farrauto, R. J. *Appl. Catal., A* **2001**, *221*, 443–457.
- (18) Bevan, D. J. M.; Kordis, J. J. *Inorg. Nucl. Chem.* **1964**, *26*, 1509–1523.
- (19) Brauer, G.; Gingerich, K. A.; Holtschmidt, U. *J. Inorg. Nucl. Chem.* **1960**, *16*, 77–86.
- (20) Campsveux, J.; Gerdanian, P. J. *Solid State Chem.* **1978**, *23*, 73–92.
- (21) Mogensen, M.; Sammes, N. M.; Tompsett, G. A. *Solid State Ionics* **2000**, *129*, 63–94.
- (22) Panhans, M. A.; Blumenthal, R. N. *Solid State Ionics* **1993**, *60*, 279–298.
- (23) Panlener, R. J.; Blumenthal, R. N.; Garnier, J. E. J. *Phys. Chem. Solids* **1975**, *36*, 1213–1222.
- (24) Riess, I.; Janczkowski, H.; Nolting, J. J. *Appl. Phys.* **1987**, *61*, 4931–4933.
- (25) Sorensen, O. T. J. *Solid State Chem.* **1976**, *18*, 217–233.
- (26) Kim, T.; Vohs, J. M.; Gorte, R. J. *Ind. Eng. Chem. Res.* **2006**, *45*, 5561–5565.

considered the equilibrium constant for differential oxidation at a particular value of x . At catalytically relevant temperatures, the $P(\text{O}_2)$ values in equilibrium with reduced ceria are so low that the fugacities must be established by equilibrium with other reactions. In a previous study, the $P(\text{O}_2)$ was established by equilibrating the oxide samples in H_2 - H_2O mixtures²⁶ and then calculating $P(\text{O}_2)$ from the equilibrium expression for H_2 oxidation, $\text{H}_2 + \frac{1}{2}\text{O}_2 \rightleftharpoons \text{H}_2\text{O}$, eq 1:

$$\log(P(\text{O}_2)) = -2 \log(K_{\text{equilibrium}}) + 2 \log [P(\text{H}_2\text{O})/P(\text{H}_2)] \quad (1)$$

To determine the average oxidation state of the $\text{CeO}_{(2-x)}$ in equilibrium with that $P(\text{O}_2)$, the amount of O_2 required for complete oxidation of the sample back to CeO_2 was measured.

For CeO_2 between 873 and 1173 K, it was possible to vary the H_2 : H_2O partial pressures in a flow system so as to obtain equilibrium constants for compositions ranging from $\text{CeO}_{1.80}$ to $\text{CeO}_{1.97}$ and the thermodynamic values obtained by this procedure were found to agree well with established literature values.²⁶ Unfortunately, each of the ceria-zirconia solutions that were examined remained substantially reduced at all $P(\text{O}_2)$ that were readily accessible using H_2 : H_2O mixtures in a flow system, making it impossible to measure equilibrium constants for the most easily removed oxygen. This is a serious limitation since the most easily removed oxygen is likely the most important for catalytic applications. It is also noteworthy that each of the ceria-zirconia samples exhibited a plateau in the oxygen stoichiometry at the higher $P(\text{O}_2)$. For example, $\text{Ce}_{0.81}\text{Zr}_{0.19}\text{O}_{1.90}$ was found to be the stable composition over a relatively wide range of $P(\text{O}_2)$, independent of temperature, at the highest values of $P(\text{O}_2)$ reasonably accessible with H_2 : H_2O mixtures obtainable in a flow system.

In the present work, we used Coulometric titration to determine the thermodynamic redox properties of ceria-zirconia solutions having the average composition of $\text{Ce}_{0.81}\text{Zr}_{0.19}\text{O}_{(2.0-x)}$ (Ce81) and $\text{Ce}_{0.25}\text{Zr}_{0.75}\text{O}_{(2.0-x)}$ (Ce25). These compositions were chosen for study so as to investigate cerium-rich and cerium-poor solid solutions in the higher $P(\text{O}_2)$ region. The results indicate that oxidation enthalpies for both samples are similar and only weakly dependent on the extent of reduction. Differences in the ease with which some oxygen is removed from the lattice appear to be associated with entropic effects related to the number of sites from which oxygen can be removed from the lattice.

Experimental Techniques

Coulometric Titration. Coulometric titration has been used by many groups to measure the redox properties of oxides;^{24,27-37}

- (27) Abrantes, J. C. C.; Perez-Coll, D.; Nunez, P.; Frade, J. R. *Electrochim. Acta* **2003**, *48*, 2761-2766.
 (28) Bakken, E.; Norby, T.; Stolen, S. *Solid State Ionics* **2005**, *176*, 217-223.
 (29) Diethelm, S.; Van herle, J. *Solid State Ionics* **2004**, *174*, 127-134.
 (30) Giddings, R. A.; Gordon, R. S. *J. Electrochem. Soc.* **1974**, *121*, 793-800.
 (31) Otake, H.; Nakamura, A.; Yamashita, T.; Minato, K. *J. Phys. Chem. Solids* **2005**, *66*, 329-334.

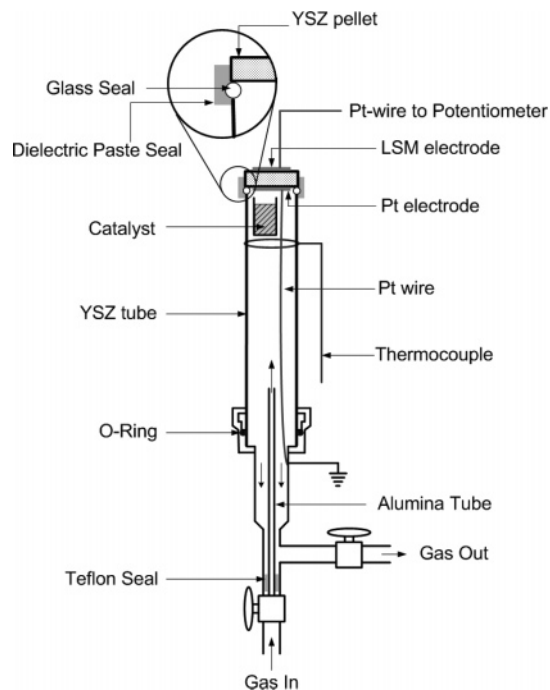


Figure 1. Schematic diagram of the Coulometric-titration cell.

however, our experimental setup, shown diagrammatically in Figure 1, has some unique features. The key component in essentially all designs is the yttria-stabilized zirconia (YSZ) pellet, produced in our case by pressing YSZ powder (Tosoh Corp., TZ-8Y, 0.2 μm) into a pellet and then firing it to 1723 K for 4 h. The pellet was 1.5 mm thick and 12 mm in diameter and was used both to electrochemically pump oxygen into the cell and to “sense” the equilibrium $P(\text{O}_2)$. Pt ink (Engelhard, A3788A) was painted onto one side of the pellet to form the inside electrode, while a 50 wt % mixture of LSM ($\text{La}_{0.8}\text{Sr}_{0.2}\text{MnO}_3$, Praxair Surface Technologies) and YSZ was applied to the other side. Both electrodes were fired to 1523 K for 4 h, and Pt wire was used to make electrical connections on both sides. The YSZ pellet was sealed to a YSZ tube (10.5% Y_2O_3 , 12.7 mm o.d., 9.5 mm i.d., and 15 cm long) using a glass powder (SCY-7, Sem-Com Company) mixed with a binder (Ceramabond, Aremco Products). After this was fired to 1223 K, the joint was coated with a dielectric paste (4461, ESL Electro-Science) and fired at 1123 K for an additional 4 h.

Only the top half of the tube with the YSZ pellet could be inserted into the furnace since the bottom of the YSZ tube was attached to a Swagelok, stainless-steel fitting with a Viton O-ring. The catalyst sample was held up near the YSZ pellet with an alumina tube so that the temperature of the sample and of the YSZ pellet could be maintained the same. Tubes welded into the Swagelok fitting allowed gases to flow over the catalyst so that the samples could be reduced at the start of the experiment. Because the $P(\text{O}_2)$ inside the YSZ tube was established by equilibrium for H_2 oxidation over most of the range of interest, the ability to flow

- (32) Otsuka-Yao-Matsuo, S.; Izu, N.; Omata, T.; Ikeda, K. *J. Electrochem. Soc.* **1998**, *145*, 1406-1413.
 (33) Park, C. Y.; Jacobson, A. J. *J. Electrochem. Soc.* **2005**, *152*, J65-J73.
 (34) Schneider, D.; Godickemeier, M.; Gauckler, L. J. *J. Electroceram.* **1997**, *1*, 165-172.
 (35) Tikhonovich, V. N.; Zharkovskaya, O. M.; Naumovich, E. N.; Bashmakov, I. A.; Kharton, V. V.; Vechev, A. A. *Solid State Ionics* **2003**, *160*, 259-270.
 (36) Tretyakov, Y. D.; Maiorova, A. F.; Berezovskaya, Y. M. In *Electrical Properties of Oxide Materials*; Trans Tec Publications: Uetikon-Zuerich, Switzerland, 1997; Vol. 125, pp 283-316.
 (37) Werner, J.; Schmidfetzter, R. *Thermochim. Acta* **1988**, *129*, 127-141.

gases into the system also allowed the initial water pressure to be increased to 10%. The Swagelok fitting was maintained at approximately 323 K with a heating tape to prevent condensation.

As mentioned earlier, the YSZ pellet was used for both oxygen pumping and sensing. A Gamry Instruments Potentiostat was used to apply a potential across the electrodes for oxygen pumping, to determine the charge transferred across the pellet (proportional to the amount of oxygen transferred) and to measure the open-circuit voltage (OCV). To avoid reduction of the YSZ pellet, the potential used for pumping oxygen was never allowed to be above 1.2 V but this was sufficient to provide 2–20 mA for pumping oxygen into the cell. A current of 1 mA corresponds to 0.16 μmol of O_2/min . At equilibrium, the OCV is related to the $P(\text{O}_2)$ through eq 2.

$$\text{OCV} = -RT/4F * \log\{P(\text{O}_2)/0.21 \text{ atm}\} \quad (2)$$

After oxygen was added to a sample, the OCV was monitored as a function of time until the potential changed by less than 1 mV/h. This time to reach equilibrium varied but typically took between 4 and 24 h. The equilibration time was a function of the sample used, $P(\text{O}_2)$, and the temperature. At 973 K, for lower $P(\text{O}_2)$, the equilibration time for $\text{CeO}_2\text{--ZrO}_2$ solid solutions was around 4–6 h, whereas for the Cu/silica sample it was around 12 h. For higher $P(\text{O}_2)$, the equilibration time was usually longer. As expected, the time for equilibrium was longer at lower temperatures because of slower kinetics to reach equilibrium.

To test for leaks, a mixture of 3% H_2O , 10% H_2 , and 87% N_2 was passed through the system, without loading a sample. When the OCV was 0.85 V, the gas flow was stopped and the OCV measured with time. The system was considered satisfactory only if the leak rate corresponded to $<1 \mu\text{mol}$ of O_2/day .

During these leak-test experiments, it was discovered that the YSZ pellet in the presence of Pt can be reduced at $P(\text{O}_2)$ corresponding to potentials above approximately 0.85 V (5×10^{-19} atm at 973 K). This was established by the fact that it was necessary to add significant amounts of oxygen into an empty cell that had been reduced to higher voltages to reduce the OCV. Similar results have been reported by others,³⁷ who suggested that the tendency to form PtZr_3 provides a thermodynamic driving force for reduction of YSZ at the Pt–YSZ interface. Unfortunately, this limiting factor made it impossible to measure equilibrium properties in the same range of $P(\text{O}_2)$ values obtained by equilibrating in flowing $\text{H}_2\text{--H}_2\text{O}$ mixtures.

Because we were unable to reduce the ceria–zirconia samples to a known oxygen to metal (O/M) ratio in the Coulometric titration apparatus and because we were unsure that the samples were completely oxidized at the end of the experiment, the absolute stoichiometries are somewhat uncertain. Since oxidation enthalpies, calculated from eq 3, require the equilibrium $P(\text{O}_2)$ to be measured as a function of temperature at fixed composition, it was necessary to ensure that we used the same starting stoichiometry at each temperature.

$$-\Delta H/R = \delta \ln P/\delta(1/T)|_{\text{O/M}} \quad (3)$$

This was accomplished by reducing samples at 973 K and allowing them to equilibrate at 973 K. The apparatus and samples were then heated to 1073 K or cooled to 873 K, with the knowledge that the stoichiometry would remain constant. Consistency between the isotherms at different temperatures was checked by making sure that the results were independent of pathway (i.e., for the addition of a known amount of oxygen, the same $P(\text{O}_2)$ was obtained at 873 K when the oxygen was added at 873 K as when the oxygen was added at 973 K followed by lowering the temperature of the system).

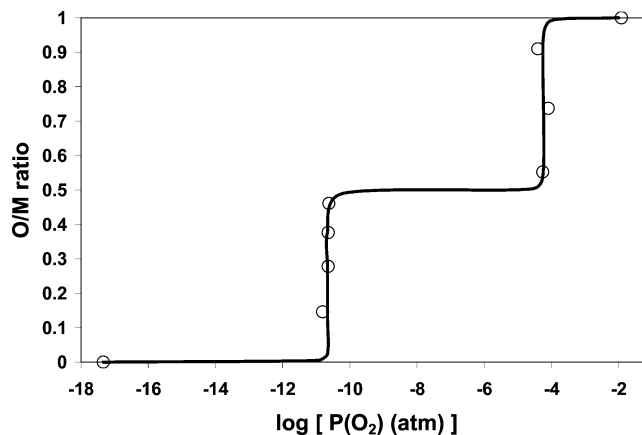


Figure 2. Oxygen to Cu ratio as a function of $P(\text{O}_2)$ at 973 K.

Validation of Titration Apparatus. A Cu/SiO₂ catalyst was used to test the performance of the Coulometric-titration apparatus. The sample was prepared by impregnation of an aqueous solution of copper nitrate ($\text{Cu}(\text{NO}_3)_2 \cdot 3\text{H}_2\text{O}$, Alfa Aesar) onto an amorphous silica powder (Ultrasil VN 3 SP). After the sample was dried, it was calcined at 723 K for 4 h to decompose the nitrate and then was crushed. The targeted Cu content was 10 wt % but the amount of oxygen required to oxidize the reduced catalyst in Coulometric-titration measurements indicated that the Cu content was 10.8 wt %.

Figure 2 shows the results for the Coulometric-titration measurements on the Cu/silica catalyst at 973 K, starting from the reduced sample. When no catalyst was placed in the system, the addition of even a single dose of oxygen was sufficient to raise the $P(\text{O}_2)$ above 10^{-2} atm. With 0.14 g of the Cu/silica catalyst in the system, the data show that there are two steps in the titration measurement. Starting from the fully reduced sample, the $P(\text{O}_2)$ rises to 2×10^{-11} atm upon the introduction of a small amount of oxygen. As more oxygen is added, the $P(\text{O}_2)$ value remains fixed at 2×10^{-11} atm until the O:Cu ratio reaches 0.5. Additional oxygen raises the $P(\text{O}_2)$ to a new value, 7×10^{-5} atm. This new $P(\text{O}_2)$ is maintained until the O:Cu stoichiometry exceeds 1.0.

The interpretation is obvious. For O:Cu stoichiometries between 0 and 0.5, there is an equilibrium between Cu and Cu_2O . The tabulated equilibrium constant for the reaction $\text{Cu}_2\text{O} = 2\text{Cu} + \frac{1}{2}\text{O}_2$, 3.4×10^{-11} atm,³⁸ agrees with our value within our ability to perform the measurement. For O:Cu stoichiometries between 0.5 and 1.0, equilibrium is established for the reaction $2\text{CuO} = \text{Cu}_2\text{O} + \frac{1}{2}\text{O}_2$. Again, our results are in good agreement with the expected value for this reaction, 5.3×10^{-5} atm.³⁸

Ceria–Zirconia Samples. Ceria–zirconia mixed oxides with composition $\text{Ce}_{0.81}\text{Zr}_{0.19}\text{O}_2$ (Ce81) and $\text{Ce}_{0.25}\text{Zr}_{0.75}\text{O}_2$ (Ce25) were prepared using the citric acid method, as described in a previous paper.³⁹ Stoichiometric amounts of $\text{Ce}(\text{NO}_3)_3$ and $\text{ZrO}(\text{NO}_3)_2 \cdot x\text{H}_2\text{O}$ were dissolved in distilled water and then mixed with aqueous citric acid ($\geq 99.5\%$, Aldrich) to produce a solution with a citric acid to total metal ions ratio of 2:1. The solution was stirred vigorously at room temperature for at least 1 h and then the water was removed by evaporation. The resulting solid was decomposed to produce the oxide by annealing in air at 723 K. X-ray diffraction (XRD) patterns were collected using a Rigaku Geigerflex diffractometer with a Cu K α radiation source ($\lambda = 1.5405 \text{ \AA}$), and the diffraction patterns for both the Ce25 and Ce81 samples calcined at 723 K were consistent with the formation of a solid solution with the given

(38) NIST WebBook. <http://webbook.nist.gov/chemistry/>, 2006.

(39) Kaspar, J.; Fornasiero, P.; Baiducci, G.; Di Monte, R.; Hickey, N.; Sergo, V. *Inorg. Chim. Acta* **2003**, *349*, 217–226.

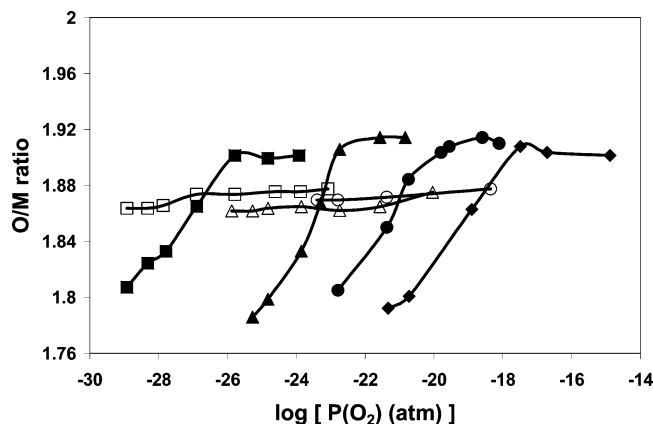


Figure 3. Oxygen to total metal (Ce + Zr) ratio of $\text{Ce}_y\text{Zr}_{1-y}\text{O}_{2-x}$ as a function of $P(\text{O}_2)$ and temperature (\square 873 K, \triangle 973 K, \circ 1073 K, \diamond 1173 K). Closed symbols: $y = 0.81$. Open symbols: $y = 0.25$. All data are from flow system experiments.

ceria content.³⁹ However, because the crystallite sizes were very small, the XRD peaks were too broad to allow definitive identification of the samples as being solid solutions.

Additional Sample Characterization. For the lower range of $P(\text{O}_2)$, the thermodynamic properties were obtained using the flow system described in a previous study.²⁶ Between 0.5 and 1.0 g of sample was placed in a quartz tubular reactor and oxidized in flowing air at the temperature of interest for 1 h. The sample was then reduced by exposure to a flowing H_2 - H_2O mixture (30 mL/min) at the desired temperature for 3 h. Water was introduced into the gas stream by passing pure H_2 through a temperature-controlled, water bubbler and the H_2O partial pressure was calculated from the vapor pressure of H_2O . After equilibration of the sample in the H_2 - H_2O mixture, the reactor was purged with dry He for 0.5 h. The extent of reduction of the sample was then determined by measuring the amount of oxygen consumed upon its reoxidation. This was accomplished by flowing air (21% O_2 and 79% N_2) over the sample at a rate of 4.3 mL/min and measuring the composition of the effluent gas from the reactor using a quadrupole mass spectrometer. The N_2 signal was used as an internal standard for determining the amount of O_2 consumed. The fact that equilibrium between the H_2O - H_2 mixtures and the oxide samples was actually attained was demonstrated by showing that the solid reached the same extent of reduction regardless of whether one started with a reduced or an oxidized sample.

Finally, because the previous study showed that large changes in the surface areas of the samples, from 2 to 30 m^2/g , had no effect on the values obtained in the thermodynamic measurements, we did not investigate the effect of surface areas in this study.

Results and Discussion

Equilibrium oxygen stoichiometries for the Ce81 and Ce25 samples at the lower $P(\text{O}_2)$ values, obtained using the flow system, are shown in Figure 3. The data for the Ce81 sample at temperatures ranging from 873 to 1173 K are simply reproduced from the previous study in our laboratory.²⁶ With use of eq 3 to calculate the partial enthalpies of oxidation, it was reported that $\Delta H = -520 \pm 20$ kJ/mol of O_2 for O:M ratios between 1.8 and 1.9. The fact that the limiting value for the O/M ratio at high $P(\text{O}_2)$ was ~ 1.9 at each of the four temperatures studied suggested that $\text{Ce}_{0.81}\text{Zr}_{0.19}\text{O}_{1.90}$ is associated with a relatively stable composition. Although the oxygen involved in the reduction of $\text{Ce}_{0.81}\text{Zr}_{0.19}\text{O}_{2.0}$ to $\text{Ce}_{0.81}\text{Zr}_{0.19}\text{O}_{1.90}$ is likely the most important for catalytic applica-

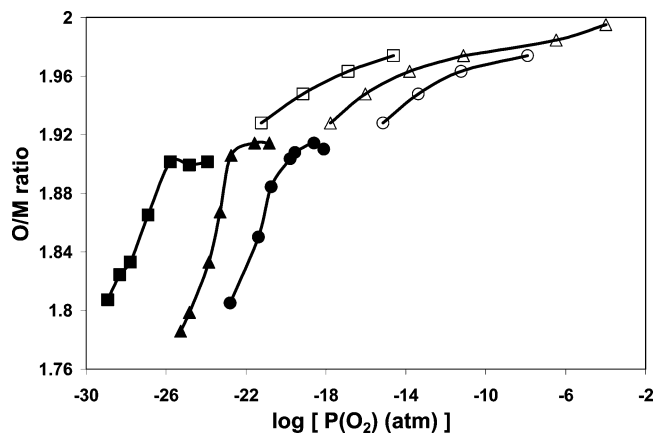


Figure 4. Oxygen to total metal (Ce + Zr) ratio for $\text{Ce}_{0.81}\text{Zr}_{0.19}\text{O}_{2-x}$ as a function of $P(\text{O}_2)$ and temperature (\square 873 K, \triangle 973 K, \circ 1073 K). Open symbols denote data from Coulometric titration. Closed symbols denote data from flow system experiments.

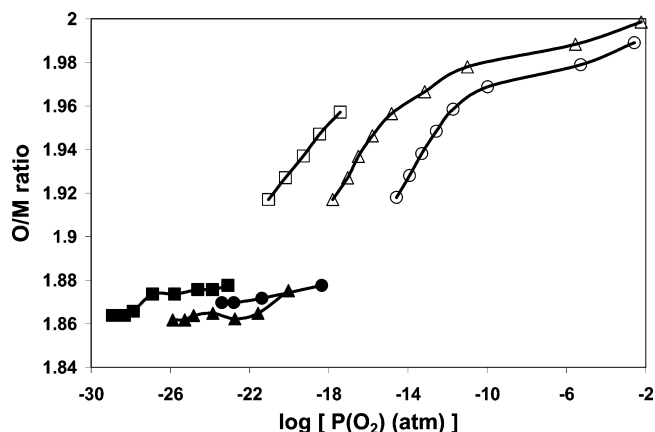


Figure 5. Oxygen to total metal (Ce + Zr) ratio for $\text{Ce}_{0.25}\text{Zr}_{0.75}\text{O}_{2-x}$ as a function of $P(\text{O}_2)$ and temperature (\square 873 K, \triangle 973 K, \circ 1073 K). Open symbols denote data from Coulometric titration. Closed symbols denote data from flow system experiments.

tions, the range of $P(\text{O}_2)$ in which the O/M ratios are between 1.9 and 2.0 was inaccessible using the flow system. Similarly for the Ce25 sample, the O:M stoichiometry remained essentially constant between 1.87 and 1.88 between 873 and 1073 K for the accessible range of $P(\text{O}_2)$ in this experiment, so that no information on oxidation enthalpies was possible. An O/M ratio of 1.875 corresponds to complete reduction of the Ce to the +3 oxidation state.

Figures 4 and 5 show the data for the Ce81 and Ce25 samples using both Coulometric titration and the flow system. The same data are tabulated in Tables 1 and 2. As discussed earlier, it was difficult to determine the absolute O/M stoichiometry for the ceria-zirconia samples using the Coulometric-titration apparatus and we have chosen to fix the O/M ratio at 2.0 for the highest $P(\text{O}_2)$ we obtained at 973 K. For both samples, the oxidation isotherms have a similar shape, suggesting that reduction of $\text{Ce}_{0.81}\text{Zr}_{0.19}\text{O}_{2.0}$ to $\text{Ce}_{0.81}\text{Zr}_{0.19}\text{O}_{1.9}$ is similar to reduction of $\text{Ce}_{0.25}\text{Zr}_{0.75}\text{O}_{2.0}$. The difference for reduction of the Ce81 sample is that there is an additional "type" of oxygen associated with reduction of $\text{Ce}_{0.81}\text{Zr}_{0.19}\text{O}_{1.9}$ to $\text{Ce}_{0.81}\text{Zr}_{0.19}\text{O}_{1.8}$.

An examination of the partial enthalpies of oxidation for the two ceria-zirconia samples, calculated using eq 3, is shown in Figure 6, together with data for pure ceria

Table 1. O/M vs $\log(P(O_2))$ Data for Ce81

temperature	flow system experiment			Coulometric titration	
	O/M	$\log(P(O_2))$ atm	H ₂ O/(H ₂ + H ₂ O) % ^a	O/M	$\log(P(O_2))$ atm
873	1.807	-28.9	0.3 ^b	1.928	-21.2
	1.824	-28.3	0.6	1.948	-19.2
	1.833	-27.8	1	1.963	-16.9
	1.865	-26.9	3	1.974	-14.6
	1.902	-25.8	10		
	1.899	-24.6	30		
	1.902	-23.9	50		
	973	1.786	-25.3	0.6	1.928
1.799		-24.8	1	1.948	-16.0
1.833		-23.9	3	1.963	-13.8
1.867		-23.3	6	1.974	-11.1
1.906		-22.7	10	1.974	-11.1
1.914		-21.6	30	1.985	-6.5
1.914		-20.8	50	2.000	-4.0
1073		1.805	-22.8	0.6	1.928
	1.850	-21.4	3	1.948	-13.4
	1.884	-20.7	6	1.963	-11.2
	1.904	-19.8	16	1.974	-7.9
	1.908	-19.6	20		
	1.914	-18.6	43		
	1.910	-18.1	57		

^a H₂O is provided by flow of pure H₂ through a bubbler of which the temperature is controlled. ^b An additional pure H₂ line is used to dilute the H₂O content.

Table 2. O/M vs $\log(P(O_2))$ Data for Ce25

temperature	flow system experiment			Coulometric titration	
	O/M	$\log(P(O_2))$ atm	H ₂ O/(H ₂ + H ₂ O) % ^a	O/M	$\log(P(O_2))$ atm
873	1.864	-28.9	0.3 ^b	1.917	-21.0
	1.864	-28.3	0.6	1.927	-20.2
	1.866	-27.9	1	1.937	-19.3
	1.874	-26.9	3	1.947	-18.5
	1.874	-25.8	10	1.957	-17.4
	1.876	-24.6	30		
	1.876	-23.9	50		
	1.878	-23.1			
	973	1.862	-25.9	0.3	1.917
1.862		-25.3	0.6	1.927	-17.0
1.864		-24.8	1	1.937	-16.5
1.865		-23.9	3	1.946	-15.8
1.862		-22.7	10	1.956	-14.8
1.865		-21.6	30	1.967	-13.2
1.875		-20.0	72	1.978	-11.0
				1.988	-5.5
				2.000	-2.2
1073		1.870	-23.4	0.3	1.918
	1.870	-22.8	0.6	1.928	-13.9
	1.872	-21.4	3	1.938	-13.3
	1.878	-18.4	50	1.948	-12.6
				1.958	-11.7
				1.969	-10.0
			1.979	-5.3	
			1.989	-2.6	

^a H₂O is provided by flow of pure H₂ through a bubbler of which the temperature is controlled. ^b An additional pure H₂ line is used to dilute the H₂O content.

calculated from the flow-titration experiments reported in an earlier paper.²⁶ The scatter in the calculated enthalpies for pure CeO₂ is partially associated with the fact that there is a change in the nature of the reduced state between 973 and 1073 K,¹⁸ near the middle of the temperature range where the isotherm experiments were performed, 873 and 1173 K. Below 973 K, an equilibrium exists between two CeO_{2-x} phases having different compositions; above 1073 K, there is only a single phase. Also, the experiments with CeO₂

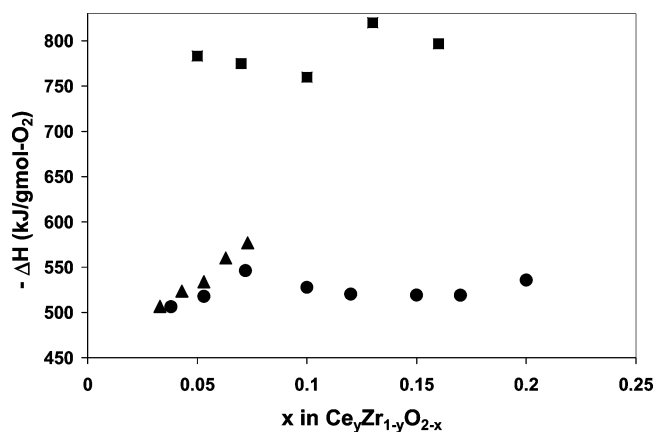


Figure 6. Partial molar enthalpy of oxidation (ΔH) at 973 K of $Ce_yZr_{1-y}O_{2-x}$ as a function of the extent of reduction. ■ $y = 1$, ● $y = 0.81$, ▲ $y = 0.25$.

suffered from the opposite problem found with the ceria–zirconia samples in the flow-titration experiments. At 873 K, it was not possible to lower the water content in the H₂, reliably and in a measurable way, so as to get significant reduction of the CeO_{2-x}. For example, at 873 K, 1.0% H₂O in 99% H₂ was more than sufficient to essentially oxidize CeO₂ completely. Therefore, the enthalpies for $x > 0.1$ were calculated using only data from 973 to 1173 K and were more strongly affected by transition in the nature of the isotherm between 973 and 1073 K. Still, the enthalpies calculated from the isotherm data are between ca. -760 and -820 kJ/mol, in good agreement with the enthalpy reported in the literature, -760 kJ/mol.⁴⁰ In agreement with at least some of the literature,¹⁸ the reduction enthalpy for CeO_{2-x} is essentially independent of x .

The partial enthalpies of oxidation for both the Ce25 and Ce81 samples range between -500 and -550 kJ/mol, with an average near -525 kJ/mol, and there are no obvious changes in the oxidation enthalpies with the extent of reduction. The values of $-\Delta H$ are lower than that obtained for pure CeO₂ by approximately 240 kJ/mol, partially explaining the comparative ease with which the solid solutions undergo reduction. However, we had anticipated that $-\Delta H$ associated with the reduction of Ce_{0.25}Zr_{0.75}O_{2.0} and the reduction of Ce_{0.81}Zr_{0.19}O_{2.0} to Ce_{0.81}Zr_{0.19}O_{1.9} would be lower than that for the reduction of Ce_{0.81}Zr_{0.19}O_{1.9} to Ce_{0.81}Zr_{0.19}O_{1.8}, whereas the data suggest that $-\Delta H$ is essentially the same for both samples and independent of O/M ratio. It is also interesting to consider that the enthalpies determined here are very close to the enthalpies of oxidation for the pyrochlore, Ce₂Zr₂O₇. Unlike ceria–zirconia solid solutions, the pyrochlore is a well-defined compound with a well-defined crystallographic structure.⁴¹ Using equilibrium data for the oxidation of the pyrochlore,³¹ we have calculated enthalpies of oxidation for this compound to be between -520 and -540 kJ/mol and, again, essentially independent of the extent of oxygen content.

The partial molar entropies of oxidation, calculated by the difference from the Gibbs free energies and the enthalpies,

(40) Lide, D. R. In *CRC Handbook of Chemistry and Physics*, Internet Version 2005 ed.; CRC Press: Boca Raton, FL, 2005.

(41) Thomson, J. B.; Armstrong, A. R.; Bruce, P. G. *J. Am. Chem. Soc.* **1996**, *118*, 11129–11133.

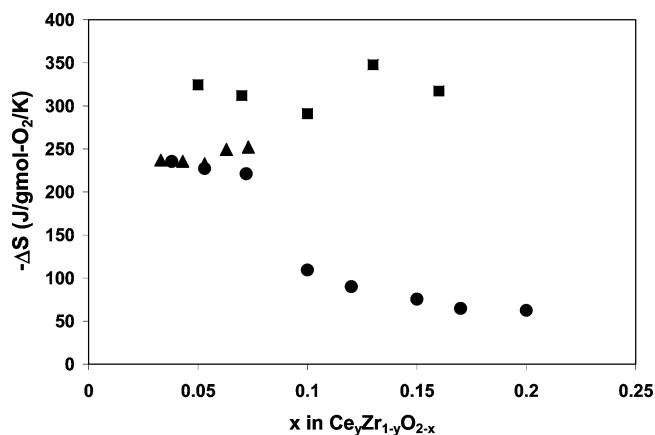


Figure 7. Partial molar entropy of oxidation (ΔS) at 973 K of $Ce_yZr_{1-y}O_{2-x}$ as a function of extent of reduction. \blacksquare $y = 1$, \bullet $y = 0.81$, \blacktriangle $y = 0.25$.

are shown in Figure 7. As expected, the entropies calculated for pure CeO_2 are once again similar to what has been reported previously, between -300 and -350 J/mol·K.^{18,21,23,25} The high entropy change for CeO_2 is due to the fact that there are a large number of sites from which oxygen can be removed since oxygen can come from anywhere in the fluorite lattice. For the reduction of the Ce25 and initial reduction of Ce81 samples, the entropy change is almost as large in magnitude as that for CeO_2 , ca. -250 J/mol·K, suggesting that oxygen can again be removed from a large number of possible sites. However, for the deeper reduction of Ce81, $Ce_{0.81}Zr_{0.19}O_{1.9}$ to $Ce_{0.81}Zr_{0.19}O_{1.8}$, the magnitude of the partial molar oxidation entropy is very low, between -50 and -100 J/mol·K, suggesting that the number of sites for oxygen removal are few. This implies that the reason for the two reduction regimes in the Ce81 sample is associated with entropic effects.

There are two main experimental observations in this study: (1) that the oxidation enthalpies for ceria–zirconia solutions having very different compositions are similar to that of the pyrochlore and different from that of pure ceria and (2) that there is a change in the number of sites from which oxygen can be removed in the Ce81 sample at a stoichiometry near $Ce_{0.81}Zr_{0.19}O_{1.9}$. To explain these, we propose viewing the reduced solid solution as a collection of “pyrochlore-like” structures, with Ce^{n+} and Zr^{4+} cations (n will be either 3 or 4 depending whether it is reduced or

oxidized) as seen in Figure 8A. In a pyrochlore lattice, the O vacancy is in the tetrahedral location between either four Zr^{4+} or four Ce^{n+} cations, most of them being between the four Zr^{4+} cations.^{41,42} In Ce81, the possibility of having four Zr^{4+} as tetrahedron ends is relatively low; hence, we suggest that O-vacancy formation in Ce81 is favored between four Ce^{n+} , i.e. $(Ce^{4+}-Ce^{3+})_2$, where the two Ce^{3+} cations are stabilized by two adjacent Zr^{4+} cations, forming a $(Ce^{3+}-Zr^{4+})_2O$ cluster, as shown in Figure 8. In the case of Ce25, the O vacancies could be possible between four Zr^{4+} or four Ce^{n+} cations.

If the energetics of oxidation is strictly local, oxidation of a cluster by adding an oxygen and oxidizing the Ce^{3+} cations to Ce^{4+} should be similar to oxidation of the pyrochlore, independent of the bulk composition, in agreement with our observations. More important, this model could explain the entropic effects observed in both the Ce25 and Ce81 samples. With the Ce81 sample, most Zr^{4+} cations can pair with several available Zr^{4+} cations and each pair of Zr^{4+} cations can interact with any pair of Ce^{4+} cations in its immediate vicinity, leading to the formation of $(Ce^{4+}-Ce^{3+})_2$ on reduction, as shown in Figure 8B. A large number of such possible combinations results in a high entropy change, similar to what is observed with pure CeO_2 . However, once each pair of Zr^{4+} cations is part of a $(Zr^{4+}-Ce^{3+})_2O$ cluster, we suggest that the number of ways in which these Zr^{4+} cations can be used in forming a second such cluster is limited, at least if there is a repulsion between oxygen vacancies; hence, the number of oxygens available for removal decreases at a stoichiometry corresponding to all of the Zr^{4+} being part of a $(Zr^{4+}-Ce^{3+})_2O$ cluster. In agreement with this picture, the plateau region of the isotherm with Ce81 occurs at a composition of $Ce_{0.81}Zr_{0.19}O_{1.9}$, which is essentially identical to the oxygen stoichiometry expected for when every Zr^{4+} cation is part of a $Ce_2Zr_2O_7$ pyrochlore-like cluster (i.e., $Ce_{0.81}Zr_{0.19}O_{1.9}$ is approximately equal to $(CeO_2)_{0.62}(Ce_2Zr_2O_7)_{0.095}$). Furthermore, the previous study of $Ce_{0.92}Zr_{0.08}O_{2.0}$ reduction showed a plateau in the isotherm at $Ce_{0.92}Zr_{0.08}O_{1.95}$,²⁶ a value that is again close to what would be expected when all of the Zr^{4+} cations are part of a pyrochlore-like cluster. With the Ce25 sample, we suggest O vacancies can form between either four Ce^{n+} or four Zr^{4+} cations, as in the pyrochlore structure. Because there are a large number of such sites, this model would predict that

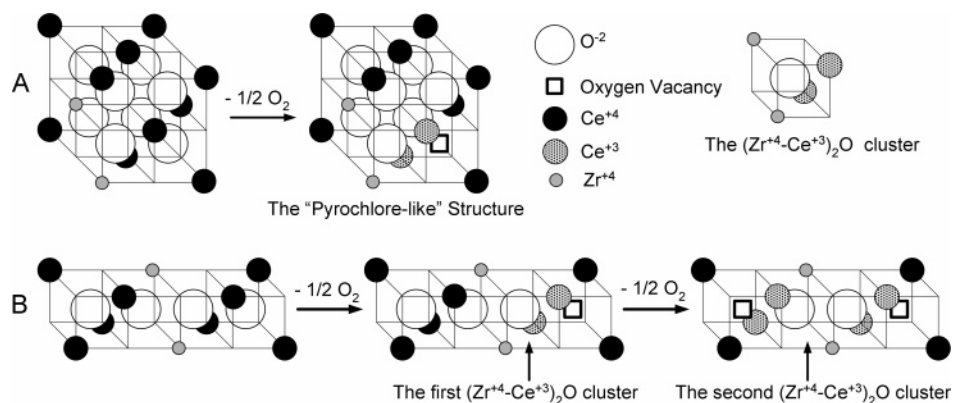


Figure 8. Schematic diagram of the proposed pyrochlore-like cluster. (A) Formation of the “pyrochlore-like” structure. (B) The two step reduction of Ce81 (only a part of the lattice structure is shown).

the oxidation entropy would remain high until complete reduction of all Ce^{4+} .

An important part of this model is that each Zr^{4+} cation can be part of at least two $(\text{Zr}^{4+}-\text{Ce}^{3+})_2\text{O}$ clusters. That this must be the case is shown by the fact that the enthalpy change for reduction of the Ce81 sample remained unchanged for O/M oxygen stoichiometries between 1.9 and 1.8.

Finally, viewing reduction of the ceria–zirconia as a localized phenomenon helps to explain the observation that temperature-programmed reduction of the solid solutions depends on the pretreatment.^{43–46} One should expect that high-temperature treatment could cause a re-ordering of the cations in the sample, with high-temperature reduction leading to a pyrochlore structure and high-temperature oxidation leading to a more random solution. Based on our results, we would not expect the energetics of reduction to

be strongly affected by changes in the ordering; however, ordering could cause large changes in the entropy of reduction.

Conclusions

The enhanced redox properties for ceria–zirconia solutions can be explained by viewing reduction of the solid in terms of “pyrochlore-like” structures, $\text{Ce}_2\text{Zr}_2\text{O}_8$ to $\text{Ce}_2\text{Zr}_2\text{O}_7$. The reduction enthalpy is approximately -525 kJ/mol O_2 , independent of oxygen stoichiometry or Ce content in the solid solutions. At least some of the changes in the reducibility of ceria–zirconias with Ce content appear to be due to entropic effects associated with the number sites that can form O vacancies.

Acknowledgment. This work was supported by the Department of Energy, Office of Basic Energy Sciences, Chemical Sciences, Geosciences and Biosciences Division. Helpful discussions with Profs. Peter Davies and Alan Jacobson are acknowledged. P.F. gratefully acknowledges financial support from CNR (Rome) – Short Term Mobility Program and FISR2002 “Nanosistemi inorganici ed ibridi per lo sviluppo e l’innovazione di celle a combustibile”.

CM061374F

-
- (42) Thomson, J. B.; Armstrong, A. R.; Bruce, P. G. *J. Solid State Chem.* **1999**, *148*, 56–62.
- (43) Baker, R. T.; Bernal, S.; Blanco, G.; Cordon, A. M.; Pintado, J. M.; Rodriguez-Izquierdo, J. M.; Fally, F.; Perrichon, V. *Chem. Commun.* **1999**, 149–150.
- (44) Fornasiero, P.; Montini, T.; Graziani, M.; Kaspar, J.; Hungria, A. B.; Martinez-Arias, A.; Conesa, J. C. *Phys. Chem. Chem. Phys.* **2002**, *4*, 149–159.
- (45) Montini, T.; Banares, M. A.; Hickey, N.; Di Monte, R.; Fornasiero, P.; Kaspar, J.; Graziani, M. *Phys. Chem. Chem. Phys.* **2004**, *6*, 1–3.
- (46) Yeste, M. P.; Hernandez, J. C.; Bernal, S.; Blanco, G.; Calvino, J. J.; Perez-Omil, J. A.; Pintado, J. M. *Chem. Mater.* **2006**, *18*, 2750–2757.